Nonlinear Coupled Dynamic Characteristics and the Stability of Rotor-Bearing System under Rub-Impact and Oil-Film Forces

Miao Jin[1, 2, a], Ailun Wang[1, 2, b], Longkai Wang[1, 2], Qike Huang[1, 2]
[1]*College of Mechanical &Electrical Engineering, Central South University, Changsha 410083, China, Hunan Province, China*
[2]*State Key Laboratory of High Performance Complex Manufacturing, Central South University, Changsha 410083, PR China*

Keywords: Rotor-bearing system, Nonlinear oil force, Rub-impact, Jump phenomenon, Stability.

Abstract: The nonlinear coupled dynamic model of a rotor-bearing system with interaction between the rub-impact and oil-film forces is established by the Lagrangian's equation and D'Alembert principle. The nonlinear coupled dynamic equation of rotor-bearing system with rub-impact and oil film force is investigated by the 4th-order Runge-Kutta method. Base on the dynamic model of rotor-bearing system, through Time domain response, shaft trajectory, phase plane and amplitude spectrum are proposed to illustrate the nonlinear coupled dynamic behaviors. then the largest Lyapunov exponent, Poincare map are identified to the stability of the obtained computational data. The excitation frequency, stator stiffness and mass eccentricity as the control parameters to study the influence of rotor-bearing system dynamics. Various nonlinear dynamic characteristics are discovered in the rotor-bearing system, such as periodic-1, multi-periodic, quasi-periodic and chaos motion are observed through the numerical simulation in this study. The numerical results indicated that coupled effects of rub-impact and nonlinear oil film force have a great influence on the vibration and instability of the rotor-bearing system as the varied excitation frequency. The nonlinear oil film force causes the oil whirl in the rotor-bearing system at the low excitation frequency. The rub-impact force mainly affects the dynamic characteristics of the high excitation frequency. The instability of rotor-bearing system occurs in the critical speed due to the instability of oil film. Larger stator stiffness can simplify the nonlinear dynamic response of system. As the stiffness of the stator increases, the system response gradually transforms from chaotic motion to period-1 motion. Under the effect of a large imbalance, jump phenomenon of system will be more obvious. and instability of system will occur in advance. The corresponding results obtained in this paper may promote to the further understanding of nonlinear dynamic behaviors of a rotor-bearing system and provide useful reference for suppressing the fault of rotating machinery.

1 INTRODUCTION

Rotating machinery, one of the most significant heavy machinery, are widely used mechanical equipment in the industrial fields(Y. Zhang and W. M.Wang, 2010). For example, such as aircraft engine, gas turbine and steam turbine are all belong to this category. As the core component of the aero-engine, the rotor-bearing system are widely used in the rotating machinery. Under the extreme condition, such as oil film force, rub-impact force, sealing force, pedestal looseness and initial bend are all belong to the multiple nonlinear exciting sources. These coupled faults can lead the rotor-bearing system to be self-excited vibration and cause the serious accidents. According to incomplete statistics (W. Li, 2002), Engine fault caused by vibration problems has accounted for 70% of total accidents. In these accidents, the fault of rotor-bearing system takes accounts for 60%-70% in the vibration fault. According to relevant reports, due to the rub-impact fault caused by engine turbine seals, four F-16 fighter jets were crashed in the United States in 1994-1995, forcing 339 flight to ground directly or indirectly(D.-y. Wang, 1998).

Due to the demand for the high rotating speed and improve the efficiency in the heavy-duty rotating machines. It is common to decrease the

Jin, M., Wang, A., Wang, L. and Huang, Q.
Nonlinear Coupled Dynamic Characteristics and the Stability of Rotor-Bearing System under Rub-Impact and Oil-Film Forces.
DOI: 10.5220/0008849101750186
In *Proceedings of 5th International Conference on Vehicle, Mechanical and Electrical Engineering (ICVMEE 2019)*, pages 175-186
ISBN: 978-989-758-412-1

radial clearance between the rotor and stator when designing a rotor-bearing system. A larger radial clearance can result the possibility of the rub-impact occurs as the excitation frequency increases. Consequently, rub-impact fault is one of main problem in the rotating machineries. the serious rub-impact fault may cause the vibration accidents of whole machine, blade break, Engine structure damage and the instability of rotor-bearing system. According to related reports, In the 1962, the second prototype of the Harrier Jet (p.1127) was in the test flight, due to rub-impact caused by the engine compressor rotor blades-casing, eventually resulted in the titanium alloy of engine to catch fire, the plane crashed on a hillside.

The traditional dynamic characteristics of rotor-bearing system mainly adopts the theoretical analysis and method of linear vibration. In the deal with many practical engineering problems, reasonable linearization can significantly reduce the computational complexity and analysis steps. However, with the rapid development of rotating machinery, nonlinear excitation sources such as oil film force, sealing force, gas excitation and thermal bending exists in the rotor-bearing system. Nonlinear exciting forces of the rotor-bearing system may present complex dynamic characteristics such as multiple solutions, jump phenomenon, subharmonic resonances, quasi-periodicityperiodic-doubling bifurcation, multiple attractors coexistence, etc (L.-H. Yang, and W.-M. Wang, 2014).

The research indicated that the rub-impact force in a dominate position and the pedestal loose is in a subordinate position. Zhang et al.(L. K. Zhang, and Z. Y. Ma, 2016) improved the nonlinear coupled bending and torsional rotor system for the hydraulic generating set and analyzed the vibration characteristics of the complex rotor-bearing system. Sun et al. established a dual-rotor system with the rub-impact considering the gyroscopic effect, and combined MHB-AFT methods with multi-harmonic balance to calculate the accuracy of each harmonic component, they analyzed the steady-state dynamic response of the multi-rotor system through the Floquet theory. Liu et al.(L. Liu and D. Q. Cao, 2015)developed the dynamic model of two rub-impacts on disk-drum-shaft rotor system using the 4th-Runge-Kutta method. The analysis results showed that the disk-drum-shaft rotor system exhibits rich nonlinear phenomena and contribute the comprehensive understanding of the dynamic behaviors about Turbo-machines. Above these researches contributed to the nonlinear dynamic behaviors of a rub-impact on rotor-bearing system.

The system is deviated from the normal state by some kind of interference. When the interference is removed, it can restore its normal state, then the system is stable. For example, in a rotating machine, a vibration whose natural frequency and rotational angular velocity are not equal. It is called oil whirl. when the speed of rotor exceeds a first-order critical speed, oil film oscillations are often accompanied in high speed rotating machinery. Due to the oil whirl frequent almost equals the amplitude of fundamental frequency. Self-exciting vibration caused by nonlinear oil film force, which will cause instability of rotor-bearing system (Q.-k. Han, and T. Yu, 2010). The frequency of self-excited vibration is non-coordinated motion. When the rotor-bearing system generates a large alternating stress, which causes the fatigue failure of the rotating shaft. There are numerous methods to identify the stability of the rotor-bearing system such as graphic method, algebraic criterion method, the largest Lyapunov exponent, center manifold theorem, and Poincare cross-section method., In these methods, the largest Lyapunov exponent and the Poincare cross-section method are beneficial to identify the dynamic behaviors of rotor-bearing system after initial disturbance. The new system generated after the initial disturbance is equivalent to the topology of original system, hence the system is stable. For example, Lee et al. (M. Lee, and J. Lee, G. Jang, 2015) determined the stability of hydrodynamic bearings with fixed grooves using finite element method(FEM) and perturbation theory. In this paper, the forced vibration and self-excited vibration were combined into a mechanical model in the complex rotor-bearing system. According to the nonlinear dynamic analysis method, the rotor-bearing system is studied by numerical integration and qualitative theory.

Of the existing work, it should be noted that the current researchers have paid closed attention to the nonlinear dynamic characteristics of rotor-bearing system with a local rubbing. But the nonlinear dynamic behaviors of rotor-bearing system with the rub-impact and oil-film forces has been seldom investigated. However, the nonlinear dynamic behaviors of rotor-bearing system are more complicated than those a sing rotor-stator contact. This paper studies on interaction with rub-impact and oil-film instability. Thus, the effect of system control parameters such as excitation frequent, stator stiffness, eccentric unbalance force are respectively discussed under the oil-film force. Finally, the jump phenomenon of the nonlinear rub-impact rotor-bearing system is investigated.

2 DYNAMIC MODEL OF SYSTEM

2.1 Mathematical Model of A Rub-Impact Rotor-Bearing System

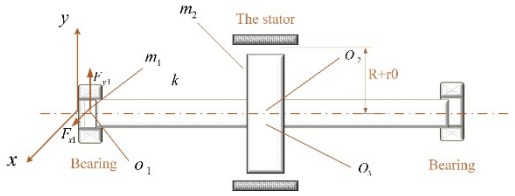

Fig 1. Model of rotor-bearing system with oil-film force and rub-impact.

A schematic model of rotor-bearing system, as illustrated in Fig.1.The rotor-bearing system consists of the disk, sliding bearing, and other attachments. O1 and O2 are the geometric center of the bearing and rotor. O3 is the center of mass of rotor. m1 and m2 are its the mass of sliding bearing and rotor disk, respectively. kc and k are the radial stiffness and the shaft stiffness, C1 and C2 are the equivalent damping coefficients of the sliding bearing and the rotor respectively. e is the mass eccentricity of rotor. $F_{x\text{-oil}}$ and $F_{y\text{-oil}}$ are the nonlinear oil film forces of the rotor-bearing system in x and y directions. The geometrical model of the rub-impact rotor-bearing system is simplified to a symmetrical rigid support according to the following assumptions:

(a) The rotor system is very complicated, the shaft is simplified as a flexible massless shaft, thermal effect, lateral torsional vibration are negligible.

(b) Rotor-bearing system are supported by Symmetrical sliding bearings and the nonlinear oil film force satisfy the Capone theory (Q.-k. Han, and T. Yu, 2010) of the short bearing.

(c) The rotor-stator is an isotropic material, and the rotor and the stator are set to be local rubbing, and the rotor is satisfied elastic deformation and Coulomb's law.

$$\begin{aligned} &m_1\ddot{x}_1 + c_1\dot{x}_1 + k(x_1 - x_2) = F_{x-oil}(x_1, y_1, \dot{x}_1, \dot{y}_1) \\ &m_1\ddot{y}_1 + c_1\dot{y}_1 + k(y_1 - y_2) = F_{y-oil}(x_1, y_1, \dot{x}_1, \dot{y}_1) - m_1 g \\ &m_2\ddot{x}_2 + c_2\dot{x}_2 + 2k(x_2 - x_1) = F_{x-rub} + mew^2\cos(wt + \varphi) \\ &m_2\ddot{y}_2 + c_2\dot{y}_2 + 2k(y_2 - y_1) = F_{y-rub} + mew^2\sin(wt + \varphi) - m_2 g \end{aligned} \tag{1}$$

2.2 Rub-Impact Force

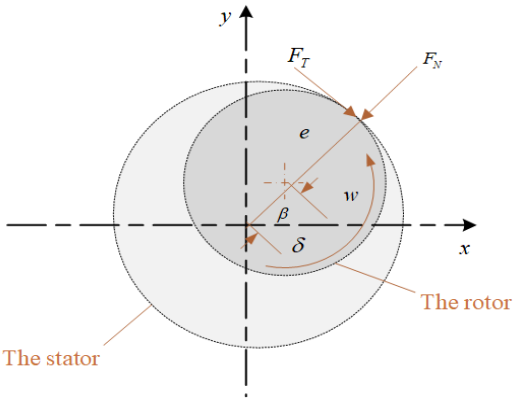

Fig 2. Rub-Impact Force.

As shown in the Fig 2, the tangential friction force and the radial friction force are approximately proportional, when a collision occurs, Rub-Impact force can be established the following equation.

$$\begin{cases} F_N = (r-\delta)k_c \\ F_T = f \cdot F_N \end{cases} \quad (r \geq \delta) \tag{2}$$

Where k_c is the stator radial stiffness, the initial clearance between the rotor and the stator is δ .and r is radial displacement of the rotor, $r = \sqrt{x_2^{\,2} + y_2^{\,2}}$

When rub-impact occurs, the rub-impact force can be written in x-y co-ordinates as:

$$\begin{Bmatrix} F_{x\text{-}rub} \\ F_{y-rub} \end{Bmatrix} = \begin{bmatrix} -\cos\beta & \sin\beta \\ -\sin\beta & -\cos\beta \end{bmatrix} \begin{Bmatrix} F_{N-rub} \\ F_{T-rub} \end{Bmatrix} \tag{3}$$

Combining equation (2) and (3), the components of the rub-impact force in the x and y directions are as follows

$$\begin{Bmatrix} F_{X\text{-}rub} \\ F_{Y-rub} \end{Bmatrix} = -\frac{(r-\delta)}{r} \begin{bmatrix} 1 & -f \\ f & 1 \end{bmatrix} \begin{Bmatrix} X_2 \\ Y_2 \end{Bmatrix} (r \geq \delta) \tag{4}$$

$$F_{X\text{-}rub} = F_{Y-rub} = 0 \quad (r < \delta)$$

2.3 Nonlinear Oil-Film Force

In this study, the oil film force has a strong nonlinearity. The nonlinear oil film force model based on the assumption of infinitely short bearing. The calculation shows that the model has better precision and convergence. The Reynolds equation

can be modified and performed as following equations:

$$\left(\frac{R}{L}\right)^2\frac{\partial}{\partial z}\left(h^3\frac{\partial p}{\partial z}\right)=X\sin\theta-Y\cos\theta-2(X'\cos\theta+Y'\sin\theta) \quad (5)$$

The dimensionless pressure can be expresses:

$$p=\frac{1}{2}\left(\frac{L}{D}\right)\frac{(X-2Y')\sin\theta-(Y+2X')\cos\theta}{(1-X\cos\theta-Y\sin\theta)^3}(4z^2-1) \quad (6)$$

Where the expression of the dimensionless oil film force in the x and y directions as follows:

$$\begin{aligned}&\begin{pmatrix}f_{x-oil}\\f_{y-oil}\end{pmatrix}=\frac{1}{\delta P}\begin{pmatrix}F_{X-oil}\\F_{Y-oil}\end{pmatrix}\\&=-A\begin{Bmatrix}3X\cdot V(X,Y,\alpha)-\sin\alpha\cdot G(X,Y,\alpha)-2S(X,Y,\alpha)\cos\alpha\\3Y\cdot V(X,Y,\alpha)+\cos\alpha\cdot G(X,Y,\alpha)-2S(X,Y,\alpha)\sin\alpha\end{Bmatrix}\end{aligned} \quad (7)$$

Where the function A , α , δ ,G,V, S are respectively given in the following equation:

$$S(X,Y,\alpha)=\frac{X\cos\alpha+Y\sin\alpha}{1-(X\cos\alpha+Y\sin\alpha)^2} \quad (8)$$

$$G(X,Y,\alpha)=\frac{2}{1-X^2-Y^2}\left[\frac{\pi}{2}+\arctan\frac{Y\cos\alpha-X\sin\alpha}{(1-X^2-Y^2)^{1/2}}\right] \quad (9)$$

$$V(X,Y,\alpha)=\frac{(Y\cos\alpha-X\sin\alpha)\cdot G(x,y,\alpha)+2}{1-X^2-Y^2} \quad (10)$$

$$A=\frac{[(X-2\dot{Y})^2+(Y+2\dot{X})^2]^{1/2}}{1-X^2-Y^2} \quad (11)$$

$$\alpha=\arctan\frac{Y+2X'}{X-2Y'}-\frac{\pi}{2}sign\left(\frac{Y+2X'}{X-2Y'}\right)-\frac{\pi}{2}sign(Y+2X') \quad (12)$$

2.4 Differential Equation of A Rub-Impact Rotor-Bearing-System Motion

The radial displacement of the rotor disk is x_2, y_2 . In order to facilitate calculation and make the rub-impact rotor-bearing-system model compliance with objective fact, eliminating the influence of dimension. The dimensionless transformations are given as follows:

$$\xi_1=\frac{c_1}{wm_1} \qquad \xi_2=\frac{c_2}{wm_2} \qquad \eta_1=\frac{k}{w^2m_1} \qquad \eta_2=\frac{2k}{w^2m_2}$$

$$\tilde{e}=e/c \qquad G=\frac{g}{cw^2} \qquad M=\frac{\delta P}{cw^2m_1} \qquad f_{y\text{-}oil}(X_1,Y_1,\dot{X}_1,\dot{Y}_1)=\frac{F_{y-oil}}{\delta p}$$

$$f_{x\text{-}oil}(X_1,Y_1,\dot{X}_1,\dot{Y}_1)=\frac{F_{x-oil}}{\delta p} \qquad X_1=x_1/c \qquad Y_1=y_1/c \qquad X_2=x_2/c$$

$$Y_2=y_2/c$$

2.5 Differential Equations of System

Defining the dimensionless time $\tau=wt$, dimensionless equation for the rotor-bearing system based on D'Alember theory can be expressed as

$$\begin{aligned}\ddot{X}_1&=-\xi_1\dot{X}_1-\eta_1(X_1-X_2)+Mf_{x\text{-}oil}(X_1,Y_1,\dot{X}_1,\dot{Y}_1)\\\ddot{Y}_1&=-\xi_1\dot{X}_1-\eta_1(Y_1-Y_2)+Mf_{y-oil}(X_1,Y_1,\dot{X}_1,\dot{Y}_1)-G\\\ddot{X}_2&=-\xi_2\dot{X}_2-\eta_2(X_2-X_1)+F_{X-rub}+\tilde{e}\cos\tau\\\ddot{Y}_2&=-\xi_2\dot{X}_2-\eta_2(X_2-X_1)+F_{Y-rub}+\tilde{e}\sin\tau-G\end{aligned} \quad (13)$$

Where the $f_{x\text{-}oil}(X_1,Y_1,\dot{X}_1,\dot{Y}_1)$ and $f_{y\text{-}oil}(X_1,Y_1,\dot{X}_1,\dot{Y}_1)$ are the dimensionless nonlinear oil film forces in x - y direction, δ is the Sommerfeld correction coefficient.

3 NONLINEAR DYNAMIC CALCULATIONS

Table 1. Relevant parameters of rotor-bearing system (units).

Parameters	valve
m_1 (kg)	4
m_2 (kg)	32
K (N/m)	2.5×10^7
Kc(N/m)	3.5×10^6
f	0.1
c_1 (N s/m)	1050
c_2 (N s/m)	2100
r_0 (mm)	0.18
G (m/s^2)	9.81
R (mm)	25
L (mm)	12
C (mm)	0.11
u	0.018
φ	0
e (mm)	0.05

The system exhibits nonlinear characteristics as control parameters such as excitation frequency, stator stiffness, mass eccentricity. The mathematical model of oil-film force has strong nonlinear

behaviors, nonlinear dynamic behaviors of the rotor-bearing system with rub-impact and oil-film forces are carried out by using 4th-RungeKutta method.

3.1 Effect of Excitation Frequency

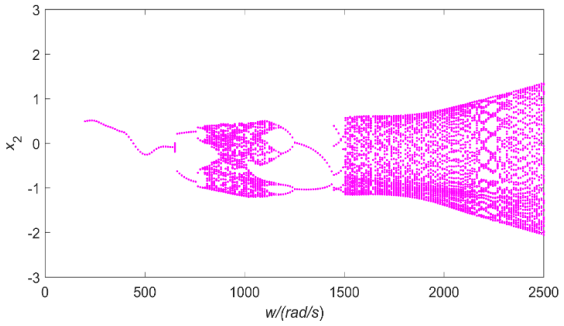

Fig 3. Bifurcation diagram of rotor-bearing system at kc=3.5×106 N/m.

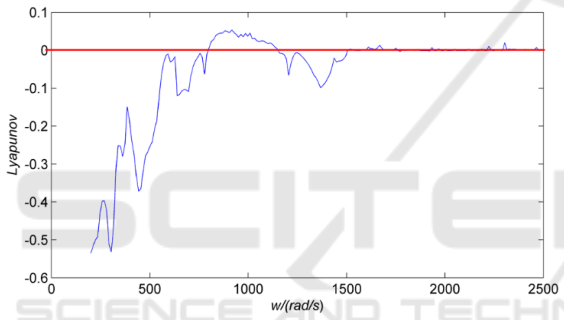

Fig 4. The largest Lyapunov exponent at kc=3.5×106 N/m.

Assume that kc= 3.5×106 N / m, e=0.050 mm, k=2.5×107 N/m, the other parameters of Rotor-bearing-system are taken from Table2. In the rub-impact process, the excitation frequency is an important parameter affecting the rotor-bearing system. The excitation frequency response curve of a rotor-bearing-system are performed by using the 4th-order Runge-Kutta method. The bifurcation diagram of rotor-bearing-system in x direction is shown in Fig.3. The corresponding value of Largest Lyapunov exponent at kc=3.5×106 N/m is shown in Fig.4.

As is shown in Fig.3, When the excitation frequency (w) is lower than 800 rad/s, the dynamic responses of the rotor is small, because the rotor and the stator have not yet rubbed. the system state is mainly dominated by the nonlinear oil film forces. When excitation frequency $w \in [200,630]$ rad/s, system keeps period-1 (P-1) motion. As is shown in Fig.5, The four figures are respectively corresponding to the Time domain response, shaft trajectory, amplitude spectrum and Poincare map. Which are used to illustrate the nonlinear dynamic behaviors of Rotor-bearing system. There is an isolated point on the Poincare map at the excitation frequency w=600 rad/s (see Fig.5). The shaft trajectory does not exceed the rub-impact boundary.

As the excitation frequency increases, the state of the rotor motion evolves from P-1 to multi-period motion at the excitation frequency $w \in [630,799]$ rad/s. when $w \in [630,750]$ rad/s for P-2 motion, $w \in [750,780]$ rad/s for P-4 motion, $w \in [780,796]$ rad/s for P-8 motion, $w \in [796,799]$ rad /s for P-16 motion. the corresponding value of the largest lyapunov exponent less than zero. It proves that the rotor-bearing system is stable. Two strange attractors appear in the Poincare map at w=850 rad/s. The amplitude spectrum shows a distinct X/2 discrete peak in fundamental spectrum. meanwhile, X/2 discrete spectrum contains continuous spectrum. And then the shaft trajectory does not exceed the rub-impact boundary. The nonlinear oil film forces are the main component in the system, resulting in a half-frequency oil whirl. The corresponding value of Largest Lyapunov exponent higher than 0 (see Fig.4). All of these give proof of that the system directly enters into chaotic motion.

When excitation frequency $w \in (1144,1495)$ rad/s. the system state undergoes an inverse period doubling bifurcation. then the system takes a series of motions $\{p16 \rightarrow p8 \rightarrow p4 \rightarrow p2\}$ (see Fig3). As the excitation frequency increases, when the $w \in (1495, 2500)$ rad/s, the rotor and the stator are collided. The rub-impact force gradually becomes the main component affecting the system response. Figure.6 represents the system is in a state of the quasi-periodic motion at the w=1800 rad/s, because the effect of gravity, the bottom boundary of the axis trajectory begins to exceed the rub-impact boundary, and a critical rub-impact occurs. the X/2 discrete peak component amplitude is significantly greater than the fundamental frequency. The frequency components of the rotor-bearing system are discrete peak with incommensurate frequencies, the corresponding value of the largest Lyapunov exponent of Fig.5 is equal to 0, and the Poincare map is a closed loop, then the oil whirl gradually becomes into the oil whip. and the system state responds to form a quasi-periodic motion.

When the excitation frequency is 2100 rad/s (see Fig.7), the bottom boundary of the axis trajectory exceeds the rub-impact boundary, and the upper boundary has a critical rub-impact occurs. the

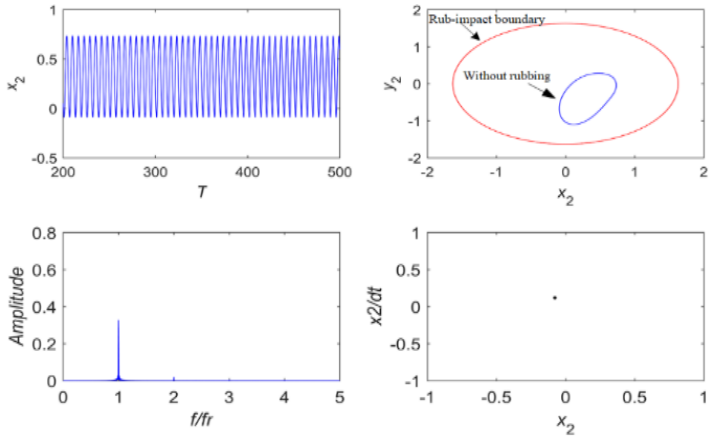

Fig 5. Time domain response, shaft trajectory, amplitude spectrum and Poincare map at w=600 rad/s.

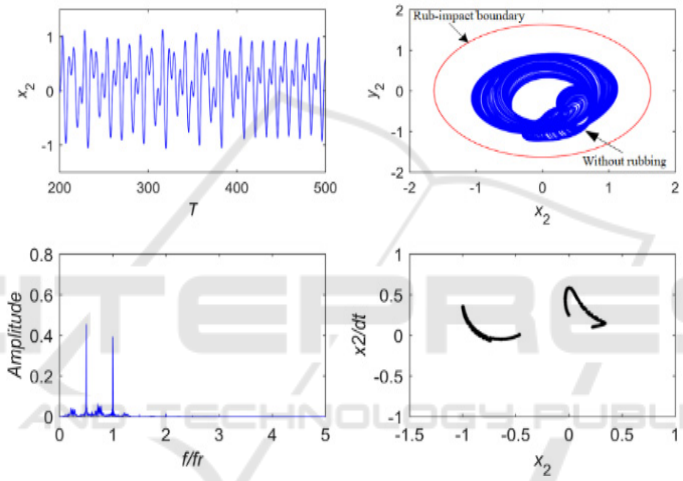

Fig 6. Time domain response, shaft trajectory, amplitude spectrum and Poincare map at w=850 rad/s.

amplitude of the X/2 discrete peak component significantly increased. Under the intercoupling of the rub-impact, the nonlinear oil film force and the unbalanced force. The effect of rub-impact is especially serious.

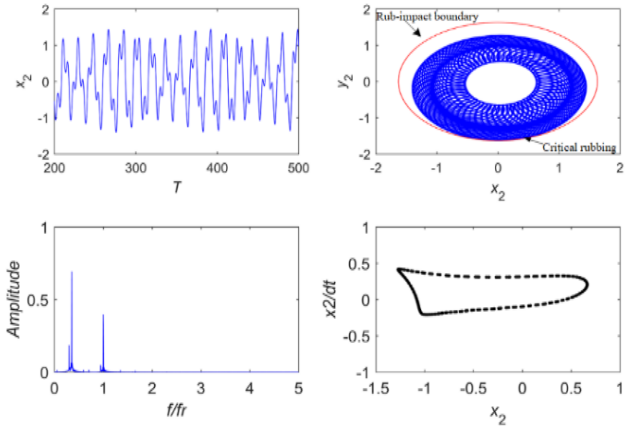

Fig 7. Time domain response, shaft trajectory, amplitude spectrum and Poincare map at w=1800 rad/s.

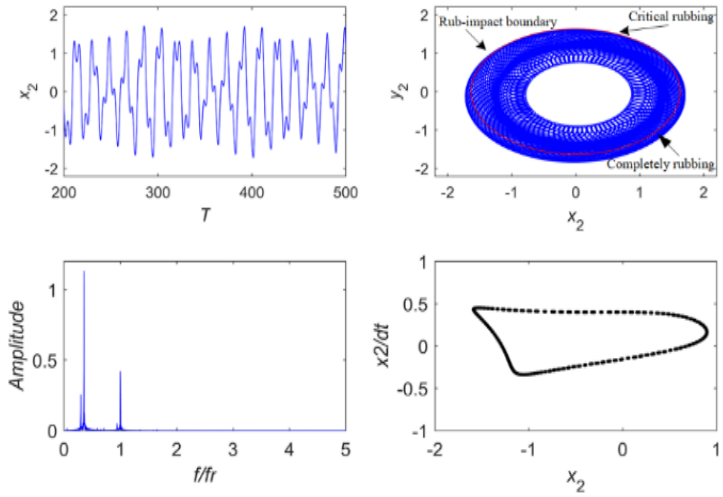

Fig 8. Time domain response, shaft trajectory, amplitude spectrum and Poincare map at w=2100 rad/s.

3.2 Influence of Stator Stiffness

In this section, when the rotor and the stator are rubbed fault, the stiffness of the stator that it plays a significant role in the nonlinear dynamic behavior of the rotor-bearing-system. Assume that w=850 rad/s, rotor clearance r0=0.04, the other parameters of Rotor-bearing-system are taken form Table 1. (Due to the rub-impact clearance is set smaller in this section, hence the rub-impact boundary is ignored). The bifurcation diagram, the Largest Lyapunuv exponent, the time domain waveform, the Poincare map, the amplitude spectrum, and the shaft trajectory are used to describe the motion of the rotor-bearing system as stator stiffness parameter changes. Fig.9 represents the bifurcation diagram of the rotor-bearing system with stator stiffness (kc) variation in the x direction at w=850 rad/s. It is observed that the nonlinear dynamic behaviors of rotor-bearing system change from the chaotic motion to periotic motion. Because the rotor displacement exists bifurcation phenomena as the stator stiffness increases linearly, therefore it takes the general forms {chaos → P-8 → P-4 → P-2 → P-1 → P-1(phase-locked). The motion of x displacement of rotor begins with chaotic motion. After a period of times, the system state gradually evolves from chaotic to multi-periodic motion. as the rub-impact force gradually replaces the nonlinear oil film force, and system finally reaches a stable P-1motion. The characteristics of states are discussed in detail below.

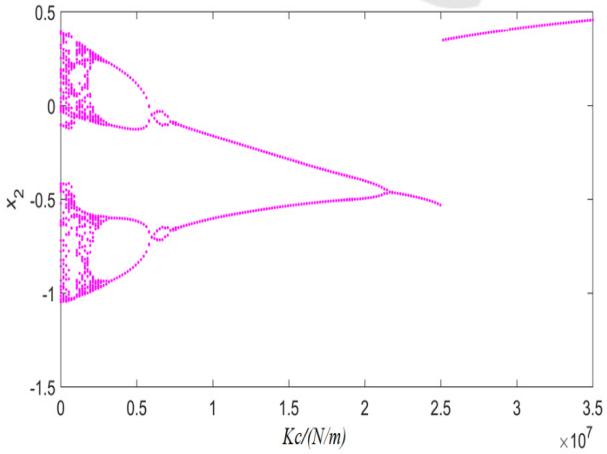

Fig 9. Bifurcation diagram of rotor-bearing-system in x direction at w=850 rad/s, r0=0.04 mm.

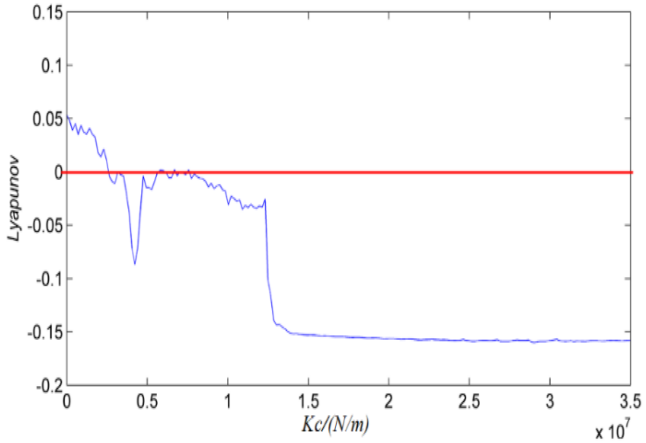

Fig 10. Largest Lyapunov exponent at w=850 rad/s r0=0.04 mm.

(1) When kc ∈ [0,0.2×107] N/m, due to the lower stator stiffness in the initial phase, the rub-impact force is much smaller than the nonlinear oil film force. It can be seen from in Fig.11, the corresponding value of Largest Lyapunov exponent is 0.054 at kc=0 N/m. Two strange attractors appear in the Poincare map. The amplitude spectrum shows a distinct X/2 discrete peak in fundamental spectrum. meanwhile, X/2 discrete spectrum contains continuous spectrum. shaft trajectory disorder. It indicates that the system is the state of chaotic motion due to the influence of oil whirl.

(2) When kc ∈ [0.2×107,2.1×107] N/m, as the stiffness of the stator increases, the rub-impact force gradually exceeds the nonlinear oil film force. System motion state experience the general forms {P-8 → P-4 → P-2} as the stator stiffness is varied. When the kc=0.7×107N/m (see Fig.12). The amplitude spectrum shows a distinct X/2 discrete peak in fundamental spectrum. there are 4 isolated points on the Poincare map. the corresponding value of Largest Lyapunov exponent is less than 0. It indicates that the motion of rotor is in a steady state.

(3) When kc > 3.1×107 N/m (see Fig.13), due to the rub-impact force far exceeds the nonlinear oil force, the system evolved from P-2 motion to P-1 motion. The shaft trajectory is oval shape and its time domain waveform is regular. The amplitude spectrum shows the high amplitude in one time frequency, indicating that the rub-impact force gradually becomes the dominant factor in the system and the phase lock is P-1 motion, which indicates that the increase of stator stiffness weakens the nonlinear behaviors of the rotor-bearing system.

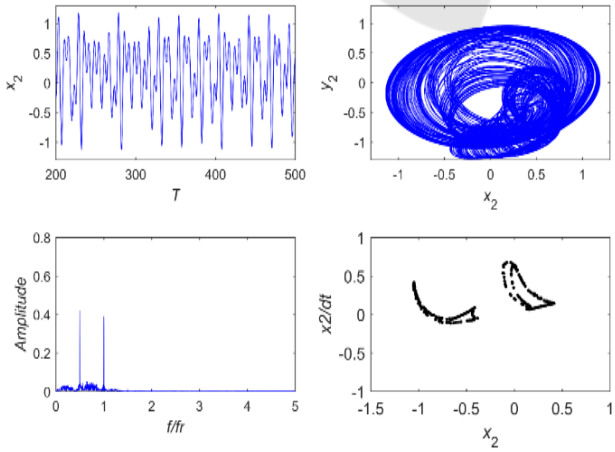

Fig 11. Time domain response, shaft trajectory, amplitude spectrum and Poincare map at kc=0 N/m.

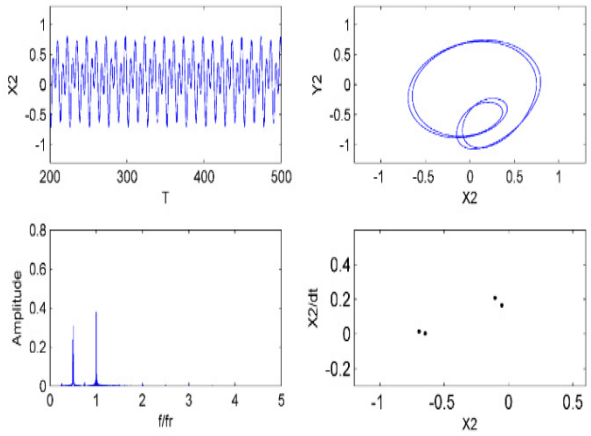

Fig 12. Time domain response, shaft trajectory, amplitude spectrum and Poincare map at kc=0 .7×107 N/m.

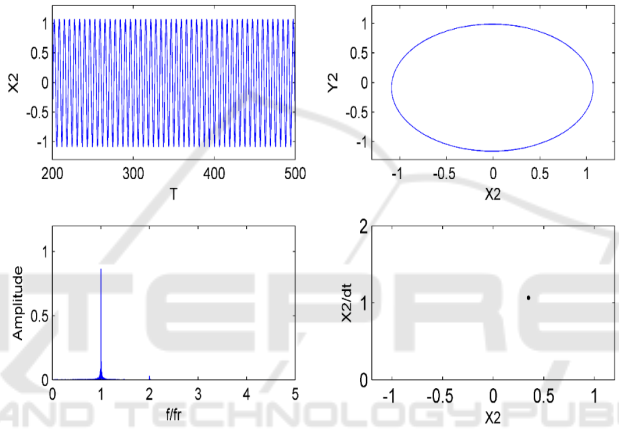

Fig 13. Time domain response, shaft trajectory, amplitude spectrum and Poincare map at kc=2.5×107 N/m.

3.3 Jump Phenomenon

In the high-pressure rotor-bearing system of a certain type of aeroengine, there has been a nonlinear vibration phenomenon since assembly. In the process of aero-engine operation, with the rotational speed increasing, the aerodynamic engine can cause the excessive vibration. that's to say, the effect of changing the rotational speed of aircraft engine. The vibration of the rotor-bearing system will be unstable and then the amplitude of rotor exists a sudden jump phenomenon when the rotor speed approaching or exceeding its 1st or 2nd order critical speed.

The vibration amplitude jumps in a short time, either from small to large, or from large to small (C. Li, and L.Shuai-ying, 2013).

With respect to this engineering problems, this section studies the dynamic characteristics of the rotor-bearing system during acceleration and deceleration section. The system parameters are taken from in Table 1. The 4th-order Runge-Kutta method is used to study the rotor-bearing system response curve.

As is shown in Fig. 14(a) (b) provides a comparison of bifurcation diagrams in the same condition (e=0.045), Overall, the dynamic characteristics exhibited by two diagrams are quite similar as (w) increases. But after the rotor passes the first-order critical speed. the rotor system responds transits from the period 2 movement to the short-term chaotic motion in the deceleration section(see Fig.14(b)). It indicates that the rotor-bearing system experiences a short-term instability after passing the critical speed range [1250, 1200] rad/s. When the eccentricity e=0.050, as shown in Fig.14(c), (d), the rotor-bearing system response experiences: {p4 → chaos → p5} at w ∈ [1350,1200] rad/s(see Fig.17(d)). Compared with e=0.045, the chaotic motion interval becomes wider. At the eccentricity e=0.055(see the Fig. 14(e) (f)), it can be seen that the system takes a series of motion:

{chaos → P-2 → chaos → P-5} in the deceleration section at w ∈ [1500,1100] rad/s(see Fig.14(f)). the system has a large jump phenomenon in this interval. Through numerical simulation, the rub-impact system will produce the jump phenomenon at a certain stage after the critical speed. As the mass eccentricity increases, the jumping phenomenon of the system will become more and more obvious, and the instability of system will occur in advance. In the process of engineering assembly, the rotor concentricity should be improved, and the eccentricity should be reduced as much as possible.

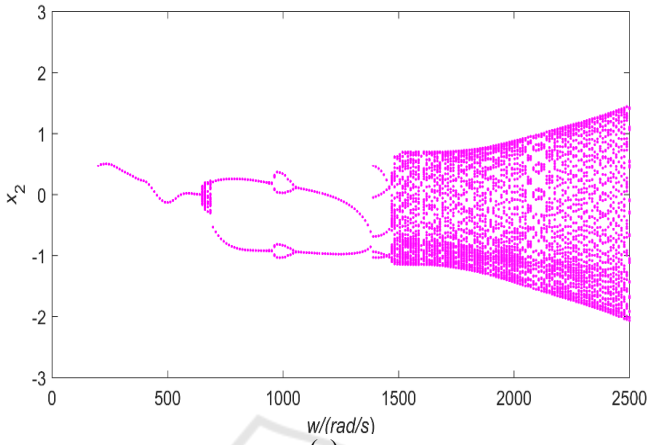

(a)

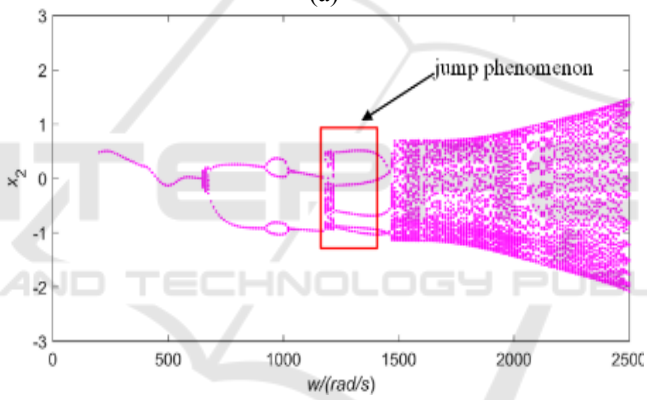

(b)

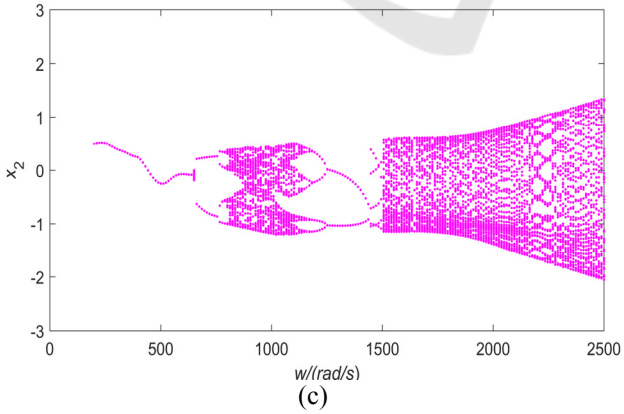

(c)

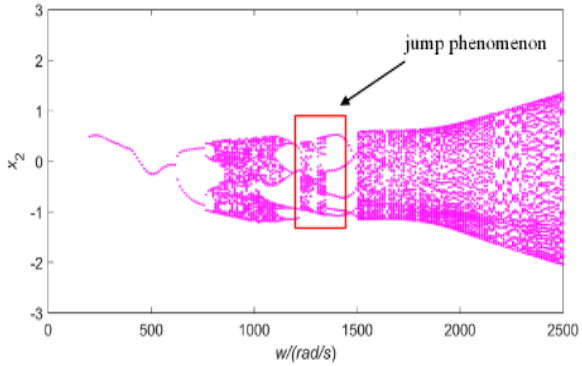

(d)

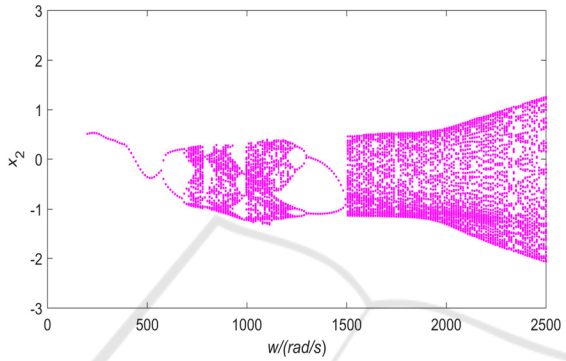

(e)

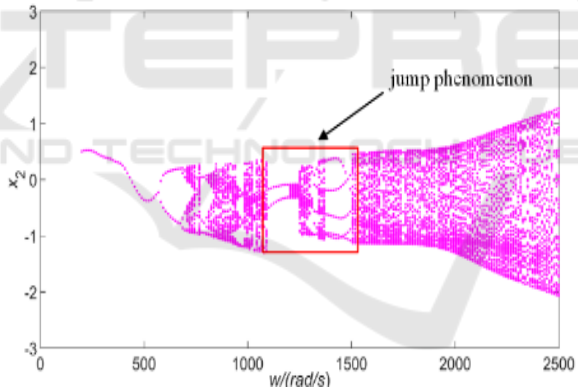

(f)

Fig 14. Bifurcation diagram of the rotor-bearing system response in x direction in certain condition :

(a) e=0.045, accelerating section, w∈[200,2500]rad/s
(b) e=0.045, decelerating section, w∈[2500,200] rad/s
(c) e=0.050, accelerating section, w∈[200,2500]rad/s
(d) e=0.050, decelerating section, w∈[2500,200]rad/s
(e) e=0.055, accelerating section, w∈[200,2500]rad/s
(f) e=0.055, accelerating section, w∈[2500,200]rad/s

4 CONCLUSIONS

In this paper, the nonlinear dynamic equation of the rotor-bearing system is established by Lagrange equation considering the rub-impact force and nonlinear oil film force. The nonlinear rotor dynamic characteristics are investigated numerical simulation. The largest Lyapunov exponent, time domain response, shaft trajectory, phase-plane, amplitude spectrum, Poincare map are applied to analyze the nonlinear vibration of rotor-bearing system. Numerical calculations indicate that the

excitation frequency, stator stiffness and mass eccentricity exist rich nonlinear characteristics for the rotor-bearing system, such as period doubling bifurcation, quasi-period and chaotic motion. Through numerical calculations, the following conclusions are obtained:

(1) The Excitation frequency has a great influence on dynamics response of rotor-bearing system. In the low excitation frequency phase, the nonlinear oil film force mainly affects the dynamic characteristic of rotor-bearing system and presents the oil film whirl. periodic- doubling, and chaotic motion can be observed through numerical calculation. When the high excitation frequency phase, the rub-impact force is mainly affecting dynamics behaviors of the rotor-bearing system. The response of rotor-bearing system is mainly based on oil film oscillation and the only the quasi-period motion can be found in the high speed.

(2) The response of rotor-bearing system is in chaotic motion at the $kc \in [0,0.2\times107]$ N/m. and the response of system is the periodic-doubling at the $kc \in [0.2\times107,2.1\times107]$ N/m. The response of rotor-bearing system responds to Phase lock for Period-1 motion at the $kc \geq 3.1\times107$ N/m. With the increases of stator stiffness is beneficial to simplify the response dynamic response of the system. the response of the rotor-bearing system gradually transforms from chaotic motion to periodic motion.

(3) In the process of acceleration and deceleration of the rotor-bearing system with rub-impact, the system exists the jump phenomenon. Under the large unbalanced condition, the jumping phenomenon of the nonlinear vibration is more obvious. In the engineering assembly, the concentricity of rotor should be increased to reduce the eccentricity as much as possible.

ACKNOWLEDGMENTS

This work is supported by the National Basic Research Program (973 Program) of china (Grant No. 2013CB035706).
The Graduate Research Innovation Project funding of Central South University (No. 2019zzts256).

REFERENCES

C. Li, L. Shuai-ying; 2013, Bistable vibration characteristics of disk-rod-fastening rotor with squeeze film dumper. Journal of Aerospace Power 28, 2044-2049 (2013).

D.-y. Wang, 1998, Rotating Machinery Rotor-Static Rubbing Vibration Characteristics. *Airspace actuator*, 37-41+36 (1998).

L.-H. Yang, W.-M. Wang, 2014, A new nonlinear dynamic analysis method of rotor system supported by oil-film journal bearings. *Appl Math Model* 38, 5239-5255.

L. K. Zhang, Z. Y. Ma, 2016, Vibration analysis of coupled bending-torsional rotor-bearing system for hydraulic generating set with rub-impact under electromagnetic excitation. *Archive of Applied Mechanics* 86, 1665-1679.

L.Liu and D. Q. Cao, 2015. Dynamic characteristics of a disk-drum-shaft rotor system with rub-impact. Nonlinear Dynamics 80, 1017-1038.

M. Lee, J. Lee, G. Jang, 2015, Stability analysis of a whirling rigid rotor supported by stationary grooved FDBs considering the five degrees of freedom of a general rotor-bearing system. *Microsyst Technol* 21, 2685-2696.

Q.-k. Han, T. Yu, 2010, *Nonlinear vibration analysis and diagnosis method for faulty rotor system*. (Science Press).

W. Li, 2002, Common Characteristics in Failure Analysis of Aeroengine Blade. *Experimental Study of Gas Turbine*, 28-30+53.

Y. Zhang, W. M. Wang, 2010, the nonlinear dynamic behavior of double-disk isotropic rotor system with rub-impact. *Mechanical Engineering and Green Manufacturing, Pts 1 and* 2, 1483-1487.